BMC Chemistry

RESEARCH

Open Access

Adsorption of Cd (II) by a novel living and non-living *Cupriavidus necator* GX_5: optimization, equilibrium and kinetic studies

Xingjie Li[1,2,3*], Qiusheng Xiao[1,2,3], Qin Shao[1], Xiaopeng Li[1,2], Jiejie Kong[1], Liyan Liu[1], Zhigang Zhao[1,2] and Rungen Li[1,3]

Abstract

Biosorbents have been extensively studied for heavy metal adsorption due to their advantages of low cost and high efficiency. In the study, the living and non-living biomass of *Cupriavidus necator* GX_5 previously isolated were evaluated for their adsorption capacity and/or removal efficiency for Cd (II) through batch experiments, SEM and FT-IR investigations. The maximum removal efficiency rates for the live and dead biomass were 60.51% and 78.53%, respectively, at an optimum pH of 6, a dosage of 1 g/L and an initial Cd (II) concentration of 5 mg/L. The pseudo-second-order kinetic model was more suitable for fitting the experimental data, indicating that the rate-limiting step might be chemisorption. The Freundlich isotherm model fit better than the Langmuir isotherm model, implying that the adsorption process of both biosorbents was heterogeneous. FT-IR observation reflected that various functional groups were involved in Cd (II) adsorption: –OH, –NH, C=O, C–O and C–C groups for the living biomass and –OH, –NH, C–H, C = O, C–N and N–H groups for the dead biomass. Our results imply that non-living biosorbents have a higher capacity and stronger strength for absorbing Cd (II) than living biomass. Therefore, we suggest that dead GX_5 is a promising adsorbent and can be used in Cd (II)-contaminated environments.

Keywords Adsorption, Cadmium, *Cupriavidus necator* GX_5, Biosorbent

Introduction

Heavy metals refer to a series of metals and metalloids with atomic numbers greater than 20 and elemental densities greater than 5 g/cm^3 [1]; heavy metals may produce devastating consequences if released into the environment. Cd is one of the most hazardous heavy metals due to its high toxicity and non-degradation [2, 3]. It has adverse effects on plant growth, animal development and microbial metabolism. Furthermore, Cd accumulation poses health risks in humans through the food chain [4], leading to skeletal dysfunctions, cancer and kidney or liver damage [5–7]. Regarding this issue, effective measures for Cd pollution disposal in soil and water must be employed to protect the environment; however, this task is challenging.

Physicochemical approaches have been extensively studied and widely used in heavy metal contaminated sites due to their advantages of short remediation time and simple operation, including ion exchange, chemical precipitation, reverse osmosis and so on [8]. However, these applications are mostly ineffective and expensive, especially those that involve low metal concentrations [9]. In contrast, the use of microbiology biomass as a

*Correspondence:
Xingjie Li
lixingjie2019@163.com
[1] College of Life Science and Environmental Resources, Yichun University, Yichun 336000, China
[2] Engineering Technology Research Center of Jiangxi Universities and Colleges for Selenium Agriculture, Yichun 336000, China
[3] Key Laboratory of Crop Growth and Development Regulation of Jiangxi Province, Yichun 336000, China

biosorption material for heavy metal remediation is an alternative method due to its low cost, high adsorption capacity and environmental friendliness [10–12].

Various types of microbiology-based biosorption materials, such as bacteria, fungi and algae, have been evaluated for their capacities to remove heavy metals [13–15]. Meanwhile, living and non-living bacterial cells have been extensively comparatively analysed for metal adsorption. Priya et al. [16] demonstrated that the biosorption of living biomass is higher than that of dead biomass. Zhu et al. [17] showed the same tendency, with adsorption capacities of 79.65 and 56.51 mg/g for living and non-living cells, respectively. In contrast, some researchers have indicated that non-living cells exhibit higher capacities than living cells [18, 19]. The biosorption procedure is a complex process that involves surface adsorption, ion exchange, chemisorption, complexation and so on [20]. In addition, it can be affected by adsorption factors, such as biomass amount, heavy metal concentrations, pH values, contact time and so on.

Although numerous bacterial cells have been studied for Cd (II) adsorption in the environment, developing a new high-capacity microbial biosorbent remains meaningful and challenging. *Cupriavidus necator* GX_5 (CP002878) is a Cd-resistant and Gram-negative bacterium formerly isolated from the rhizosphere soil of a local dominant plant near a Pb–Zn ore and considered as a plant-growth promoting rhizobacterium, which can assist hyperaccumulators to remediate Cd contaminated soil [21]. However, it is also considered a potential microbial biosorbent for Cd-polluted soil or water [22, 23]. The colony morphology is displayed in Additional file 1: Fig. S1. To our knowledge, equilibrium and kinetic studies of living and non-living *C. necator* GX_5 for Cd biosorption have not been investigated. Therefore, the present work aims to (1) analyse the biosorption potential of living and non-living biomass of *C. necato*r GX_5 as a biosorbent, (2) optimise the parameters involved in Cd removal efficiency, (3) evaluate kinetic and equilibrium models and (4) characterise both living and non-living biosorbent surfaces using scanning electron microscopy (SEM) and Fourier transform infrared spectroscopy (FT-IR).

Materials and methods

Bacterial cultivation and preparation of biosorbents

The strain of *C. necator* GX_5 was incubated in a Luri–Bertani broth medium at a pH of 7.0 ± 0.2 on a rotary shaker at 180 rpm and 28 °C until the logarithmic growth period, reaching an OD_{600} of approximately 1.0. For the living biosorbents, the biomass was collected by centrifuging at 10,000 rpm for 10 min. It was then washed three times with sterile distilled water, pre-cooled at − 80 ℃ and lyophilised 24 h with a Labconco freeze drier [24]. Thereafter, the dried pellet was ground into powder before use. For the non-living cells, the living bacterial suspension was inactivated using a high-pressure steam sterilization [25]. Dead biosorbent was prepared similarly to the abovementioned methods for the live ones. Meanwhile, the biosorbent dosages (concentrations) were calculated by grams per litre.

Cd solutions

A 1000 mg/L stock Cd solution was made by dissolving $CdCl_2{\cdot}2.5H_2O$ in double distilled water. The solution was appropriately diluted to the specified concentrations according to the adsorption experiment and sterilised before use. The pH values were also adjusted by adding 1 mol/L of HCl or NaOH. All reagents used in the experiments were analytical grade and purchased from Aladdin Biochemical Technology Co., Ltd., Shanghai, China. The purity of $CdCl_2{\cdot}2.5H_2O$ and NaOH were 99% and 98%, respectively. The mass fraction of HCl was 36–38%, corresponding to 12 mol/L.

Batch adsorption experiments

The adsorption capacity and/or removal efficiency of both the living and non-living biosorbents of *C. necator* GX_5 for Cd (II) were performed in batch experiments. They were conducted in 50 mL Erlenmeyer flasks containing 20 mL of Cd (II) working solution at 28 ℃ and a shaking speed of 180 rpm on a rotary shaker. The following influencing factors were evaluated: pH (3–7), biosorbent dosage (0.2–4 g/L), initial Cd (II) concentration (5–200 mg/L) and contact time (5–360 min). Other factors were kept constant (pH of 6, dosage of 1 g/L, initial Cd (II) concentration of 50 mg/L and contact time of 24 h). After adsorption, the supernatant was obtained by centrifuging the mixture at 10,000 rpm for 10 min. It was filtered through an inorganic filter membrane (0.22 μm), and Cd (II) concentration in the supernatant was assayed by graphite furnace atomic absorption spectroscopy (GF-AAS) AA800 (Perkin Elmer, USA). It was equipped with a graphite furnace, Zeeman correction, a hollow cathode lamp, and an air-acetylene burner [26]. The working current and wavelength were 4 mA and 228.8 nm, respectively. The instrument was controlled by a computer with WinLab32 software.

The adsorption capacity (q_e) of the biosorbents was calculated using Eq. (1) [27]:

$$q_e = \frac{(C_0 - C_e) \times V}{m} \tag{1}$$

where q_e (mg/g) defines the adsorption capacity of the biosorbent per unit; c_0 (mg/L) refers to the initial Cd (II) concentration; c_e (mg/L) represents Cd (II) concentration at equilibrium or a certain time; V (L) denotes the

volume of the working solution; and m (mg) represents the dry weight of living or non-living biomass.

The removal efficiency (*%removal*) was listed in Eq. (2) [27]:

$$\%removal = \frac{C_0 - C_e}{C_0} \times 100 \quad (2)$$

where c_o (mg/L) and c_e (mg/L) indicate the same meaning as in Eq. (1). All experiments were tested in three repetitions.

Biosorption kinetic studies

In the biosorption kinetic studies, the samples were collected, and the Cd (II) concentration in the supernatant was assayed at different time intervals (5, 10, 20, 30, 60, 120, 240 and 360 min). Other parameters remained unchanged (pH of 6, dosage of 1 g/L and initial Cd (II) concentration of 50 mg/L). The experimental data were fitted using pseudo-first-order and pseudo-second-order kinetic models.

The linear pseudo-first-order kinetic model was provided in Eq. (3):

$$\ln (q_e - q_t) = \ln q_e - k_1 t \quad (3)$$

where q_e (mg/g) and q_t (mg/g) signify the adsorption capacity of the biosorbents at equilibrium and any given time, respectively; and k_1 is rate constant. The value of k_1 was obtained from the plot of $\ln (q_e - q_t)$ versus t [28].

The linear pseudo-second-order kinetic model was expressed as:

$$\frac{t}{q_t} = \frac{1}{q_e^2 k_2} + \frac{t}{q_e} \quad (4)$$

where q_e (mg/g) and q_t (mg/g) mean the same as in Eq. (3); and k_2 implies the pseudo-second-order rate constant, which was determined by the plot of $\frac{t}{q_t}$ versus t [29].

Biosorption isotherm studies

The widely used biosorption isotherms, namely, Langmuir and Freundlich isotherm models, were adopted to study the adsorption processes of living and non-living *C. necator* GX_5 biosorbents for Cd (II) at a pH of 6.0, a dosage of 1 g/L and varying initial Cd (II) concentrations (5, 10, 20, 50, 100 and 200 mg/L). The experiment was also conducted in 50 mL sterile flasks, each with 20 mL of working solution. After adsorption for 6 h, the Cd (II) concentration in the supernatant was measured based on the previously mentioned method.

The linear Langmuir isotherm model was represented as:

$$\frac{C_e}{q_e} = \frac{C_e}{q_{max}} + \frac{1}{K_L q_{max}} \quad (5)$$

where C_e (mg/L) represents the equilibrium metal concentration; qe (mg/g) indicates the adsorption amount per unit biosorbent; q_{max} (mg/g) denotes the maximum theoretical adsorption capacity; and K_L is the Langmuir isotherm constant. The K_L and q_{max} values were calculated from the slope and intercept of the linear plot of $1/q_e$ versus $1/C_e$ [30]. To determine the favourability of the adsorption process, we calculated the dimensionless separation factor R_L using Eq. (6) [31]:

$$R_L = 1/(1 + K_L C_0) \quad (6)$$

where $R_L > 1$ indicates the adsorption process unfavourable; $R_L = 1$ indicates linear; $0 < R_L < 1$ indicates favourable; and $R_L = 0$ indicates irreversible [32].

The linear Freundlich isotherm model was written as:

$$\log q_e = \log K_F + \frac{1}{n} \log C_e \quad (7)$$

where C_e (mg/L) and q_e (mg/g) have the same meaning as in Eq. (5); K_F and n are the Freundlich isotherm constants, which were determined by the slope and intercept of the linear plot of $\log q_e$ versus $\log C_e$ [33].

SEM and FT-IR characterisation of the biosorbents

The surface morphological characteristic changes of both living and non-living biosorbents loaded with and without 100 mg/L of Cd (II) were determined by SEM (Sirion 200, USA). The strain suspension was prepared, washed and fixed with 2.5% glutaraldehyde at 4 ℃ overnight. The suspension was then smeared on a coverslip of appropriate size, air dried, dehydrated with ethanol of gradient concentrations (30%, 50%, 70%, 90% and 100%) and sputter coated with gold before observation [34].

The main functional groups before and after 100 mg/L of Cd (II) adsorption were analysed by a (FT-IR, Nicolet 6700, USA). The dried biosorbent was mixed with KBr (1:100), thoroughly ground in an agate mortar, pressed to transparent discs and immediately evaluated in the range of 4000–400 cm^{-1} at a resolution of 4 cm^{-1} [35].

Statistical analysis

Data analyses were conducted using SAS 8.1. All plots were constructed using Sigmaplot 12.5. The data were evaluated using ANOVA and the least significant difference test, with a significance set at $p < 0.05$.

Results and discussion

Effect of adsorption parameters on biosorption

The effects of solution pH in the range of 3 to 7 on Cd (II) biosorption by the living and non-living biosorbents were

studied at an initial Cd (II) concentration of 50 mg/L, dosage of 1 g/L and reaction time of 24 h. As shown in Fig. 1; Table 1, when the pH was increased from 3 to 6, the biosorption capacity of both biosorbents significantly increased and then significantly decreased for living cells at 7. Therefore, the optimal pH was considered as 6. This result may be due to the decreased competition between Cd (II) and hydroxonium ions in the solution [36]. These results agree with many other Cd (II) adsorption studies using bacterial adsorbents, which have considered 6 as the optimum pH [37, 38]. However, some researches mentioned that the maximum adsorption of Cd (II) occurs at a pH of 5 [39, 40]. In general, a pH in the range of 3 to 6 is favourable for metal adsorption by microbial adsorbents [41]. Besides, the adsorption capacity of the dead biomass was significantly higher than that of the live biomass (Table 1).

Considering that hydroxyl ions react with Cd (II) and form hydroxide sediment if the pH is higher than 7, only pH values from 3 to 7 were utilised in the study. Meanwhile, in other experiments, the maximum adsorption capacity or highest removal efficiency of the biosorbents was obtained when the pH of the solution was fixed at 6. Solution pH is a vital factor affecting biosorption because it influences the surface charges and functional groups on the active sites of the biosorbents [42].

Initial metal concentration and biosorbent dosage were the other two major factors influencing the adsorption capacity and removal efficiency of the biosorbents. As shown in Fig. 2, Additional file 1: Tables S1, S2, when the initial Cd (II) concentration was increased from 5 mg/L to 200 mg/L, the adsorption capacity of the living and non-living biomass increased from 3.03 mg/g to 17.17 mg/g and from 3.93 mg/g to 17.55 mg/g, respectively. However, for the adsorption capacity of the live biomass, there existed no difference between initial metal concentration of 5 and 10 mg/L, and between 10 and 20 mg/L, while there was a significant difference between each other when the concentration was 50, 100 and 200 mg/L. For the dead biomass, the adsorption capacity was significantly different between each two concentrations from 5 to 200 mg/L, except between 10 and 20 mg/L (Additional file 1: Table S1). The biosorption capacity of dead cells seemed higher than that of the living cells (Fig. 2),

Table 1 The effect of pH on the adsorption capacity of *Cupriavidus necator* GX_5

Biosorbents	Adsorption capacity (mg/g)				
	pH				
	3.0	4.0	5.0	6.0	7.0
Live	2.32^{f}±0.21	4.65^{e}±0.37	6.49^{c}±0.36	7.46^{b}±0.48	6.62^{c}±0.41
Dead	5.66^{d}±0.32	7.81^{b}±0.31	9.10^{a}±0.44	9.63^{a}±0.47	9.12^{a}±0.38

Note: Values are the means of three replications ± standard deviation;

Means with the same superscript letter are not significantly different ($p < 0.05$)

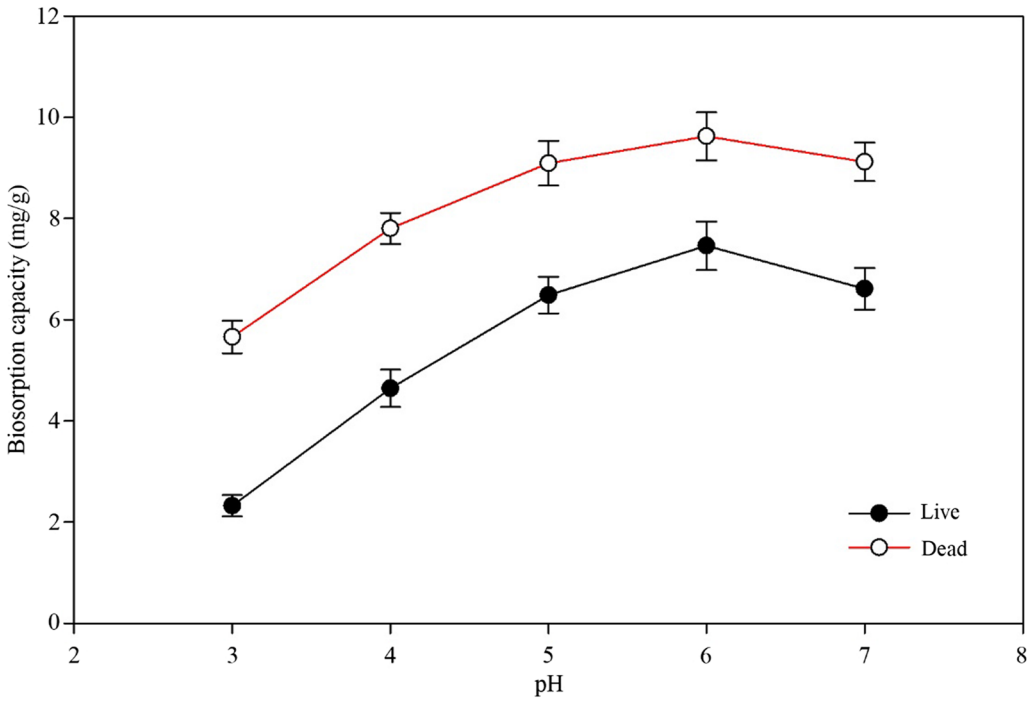

Fig. 1 Effect of pH on the adsorption capacity of *Cupriavidus necator* GX_5

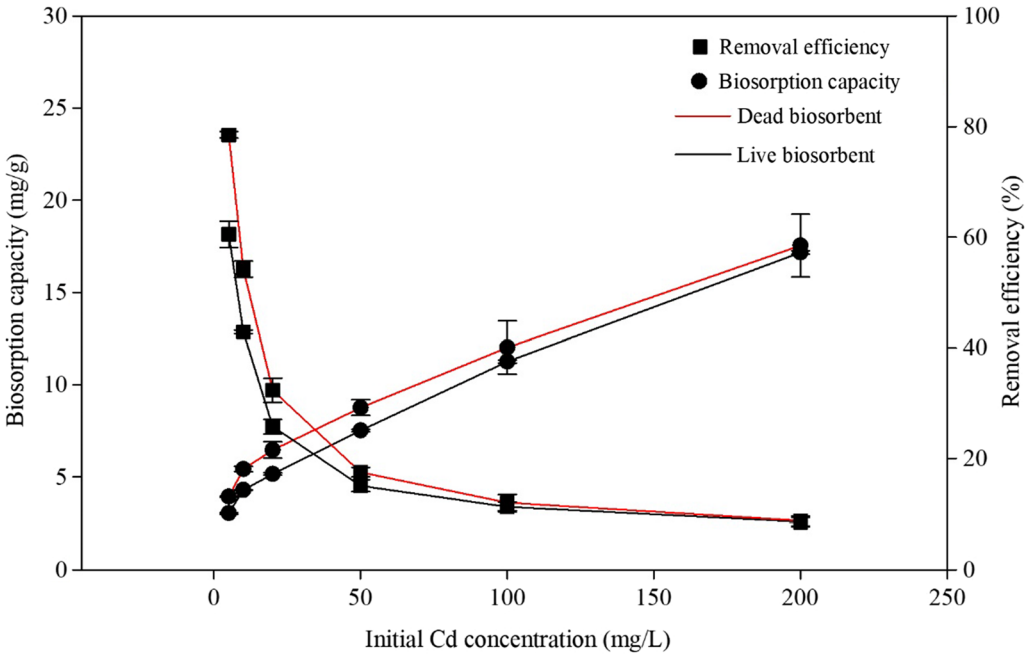

Fig. 2 Effect of initial Cd (II) concentration on theadsorption capacity and removal efficiency of *Cupriavidus necator* GX_5

but there was no significant difference (Additional file 1: Table S1).

Moreover, the removal efficiency of living and non-living biomass decreased from 60.51 to 8.58% and from 78.53 to 8.77%, respectively, and existed significant difference between each two Cd (II) concentration. Furthermore, the removal efficiency of the dead biosorbent was significantly higher than that of the live biosorbent when metal concentration was 5, 10, 20 and 50 mg/L, but with no difference at 100 and 200 mg/L, as shown in Additional file 1: Table S2. At a low concentration, sufficient binding sites were observed on the biosorbent surface, assuring that a thorough combination of Cd (II) and the biomass occurred, leading to high removal efficiency [43]. However, the ratio of metal numbers versus the available sites increases with metal concentration; therefore, the binding sites can be completely utilised, which results in improved adsorption capability [44]. Besides, the slope of the removal efficiency curve for both living and non-living biosorbents of *C. necator* GX_5 decreased at 50 mg/L of Cd (II). Therefore, this concentration was used in other batch experiments.

The effect of the dosage of living and non-living biosorbents on Cd (II) adsorption was investigated at an initial metal concentration of 50 mg/L, a pH of 6 and a reaction time of 24 h. As demonstrated in Fig. 3 and Additional file 1: Table S3, a decrease in adsorption capacity from 15.97 mg/g to 4.39 mg/g for the living biomass and from 21.47 mg/g to 5.44 mg/g for the non-living biomass occurred with an increased dosage from 0.2 g/L to 4 g/L. The adsorption capacity of the dead cells for Cd (II) was significantly different between each two dosages in the range of 0.2 to 4 g/L. But it was more complex for the living cells. And the dead pellet had a significantly higher adsorption capacity than live pellet at lower dosage of 1.2 to 1 g/L (Additional file 1: Table S3).

Conversely, the removal efficiency increased from 6.39 to 35.15% and from 8.59 to 43.49% for the living and non-living biosorbents, respectively. Unlikely to the presentation of the adsorption capacity, the removal efficiency between any two dosages of both live and dead biosorbents was significantly different as demonstrated in Additional file 1: Table S4. Similarly, the removal efficiency of Cd (II) by the dead pellet was significantly higher than live pellet. The increase in biosorbent dosage may aggregate or overlap, which means reducing the available binding sites, leading to decreased adsorption capacity [45]. The active sites on the cell surface cannot be fully applied, which has also decreased the adsorption capacity of the biosorbents [46]. However, the total site quantities in higher dosages were much greater than those in lower biomass concentrations, which can adsorb more metal ions, thus increasing removal efficiency [47]. Many other biosorbents for metal adsorption have displayed the same tendency [48–50]. Similarly, the slope of the biosorption capacity curve for both biosorbents decreased at 1 g/L. Therefore, the optimum dosage was 1 g/L, which was exploited in the experiments.

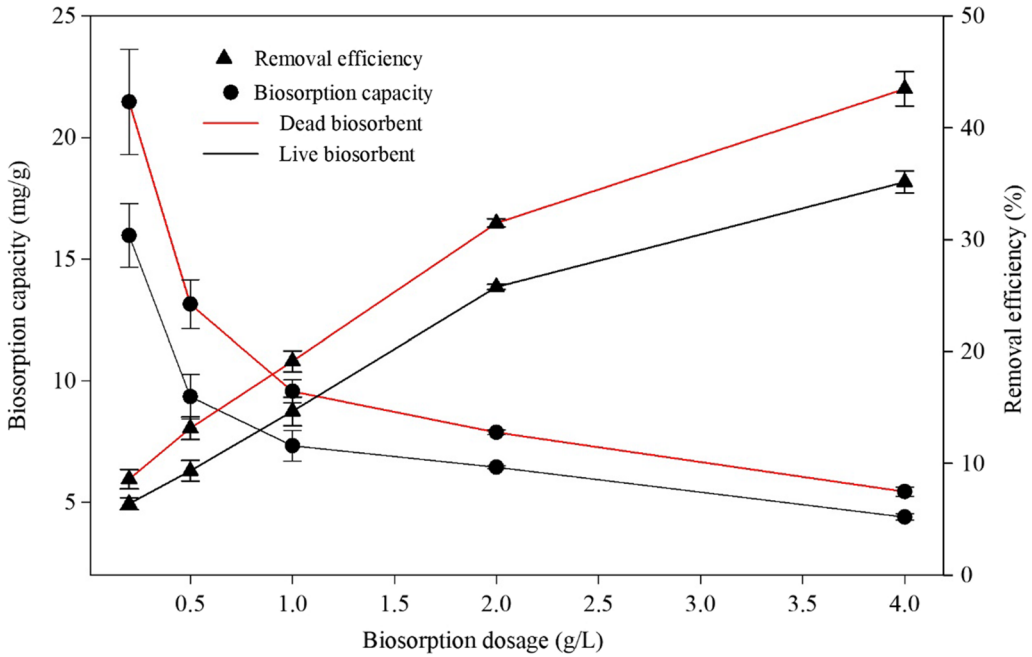

Fig. 3 Effect of dosage on the adsorption capacity and removal efficiency of *Cupriavidus necator* GX_5

Contact time was another important factor affecting the adsorption process. It determines the equilibrium time. The effects of contact time varying from 5 to 360 min on the biosorption capacity of the two biosorbents for Cd (II) were analysed, and the results are demonstrated in Fig. 4; Table 2. The adsorption capacity increased sharply in the first 30 min and reached adsorption equilibrium within 60 min. The rapid change in adsorption capacity in 30 min may be attributed to the many free available sites on the surface of

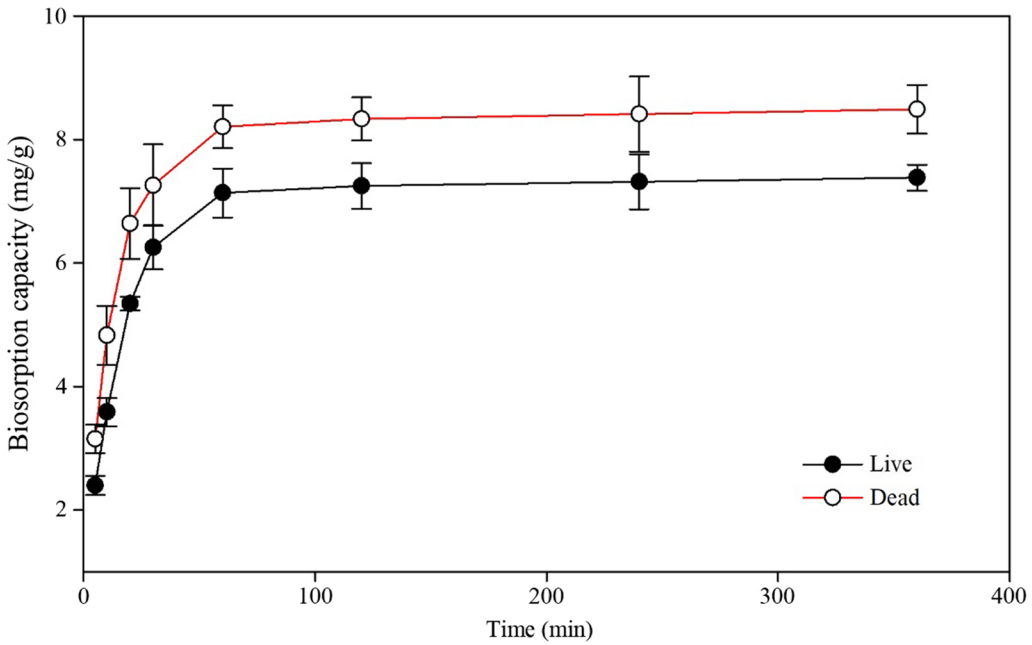

Fig. 4 Effect of contact time on the adsorption capacity of *Cupriavidus necator* GX_5

Table 2 Effect of the contact time on the adsorption capacity of *Cupriavidus necator* GX_5

Biosorbents	Adsorption capacity (mg/g)							
	Time (min)							
	5	10	20	30	60	120	240	360
Live	$2.40^{g}\pm0.16$	$3.59^{f}\pm0.23$	$5.34^{e}\pm0.11$	$6.25^{d}\pm0.36$	$7.14^{bc}\pm0.40$	$7.25^{bc}\pm0.37$	$7.32^{b}\pm0.45$	$7.38^{b}\pm0.21$
Dead	$3.15^{f}\pm0.23$	$4.83^{e}\pm0.48$	$6.64^{cd}\pm0.57$	$7.26^{bc}\pm0.66$	$8.21^{a}\pm0.35$	$8.34^{a}\pm0.35$	$8.41^{a}\pm0.61$	$8.49^{a}\pm0.39$

Note: Values are the means of three replications ± standard deviation;

Means with the same superscript letter are not significantly different ($p < 0.05$)

the biosorbents [51]. In the adsorption process, the site numbers become finite, and the presence of competition of metal ions decreases the adsorption rate until equilibrium [52].

The rate of adsorption capacity of the living (6.35 mg/g) and non-living biomass (7.26 mg/g) at 30 min occupied 86.00% and 86.84% and 7.27 mg/g and 8.36 mg/g towards the equilibrium adsorption capacity, respectively. Other researchers have reported similar results [53, 54]. Just as discussing the effects of pH, dosage and initial metal concentration on the adsorption capacity, the dead biomass was significantly higher than live biomass at any time point of the same sampling time, as displayed in Table 2.

Biosorption kinetic evaluation

To elucidate the Cd (II) adsorption process using the living and non-living *C. necator* GX_5 biomass, we tested the experimental data using the pseudo-first-order and pseudo-second-order kinetic models, which have been extensively used in metal adsorption experiments by biosorbents [55–58]. In the linear plot of ln $(q_e - q_t)$ versus t, with the reaction time proceeding, q_t is infinitely close to q_e. Therefore, this equation is applicable only to the process before adsorption equilibrium [59]. Thus, only the experimental data before 60 min were employed to fit the parameters in the equation. Figure 5; Table 3 show that the R^2 values of the pseudo-first-order and pseudo-second-order models were all above 0.99 for

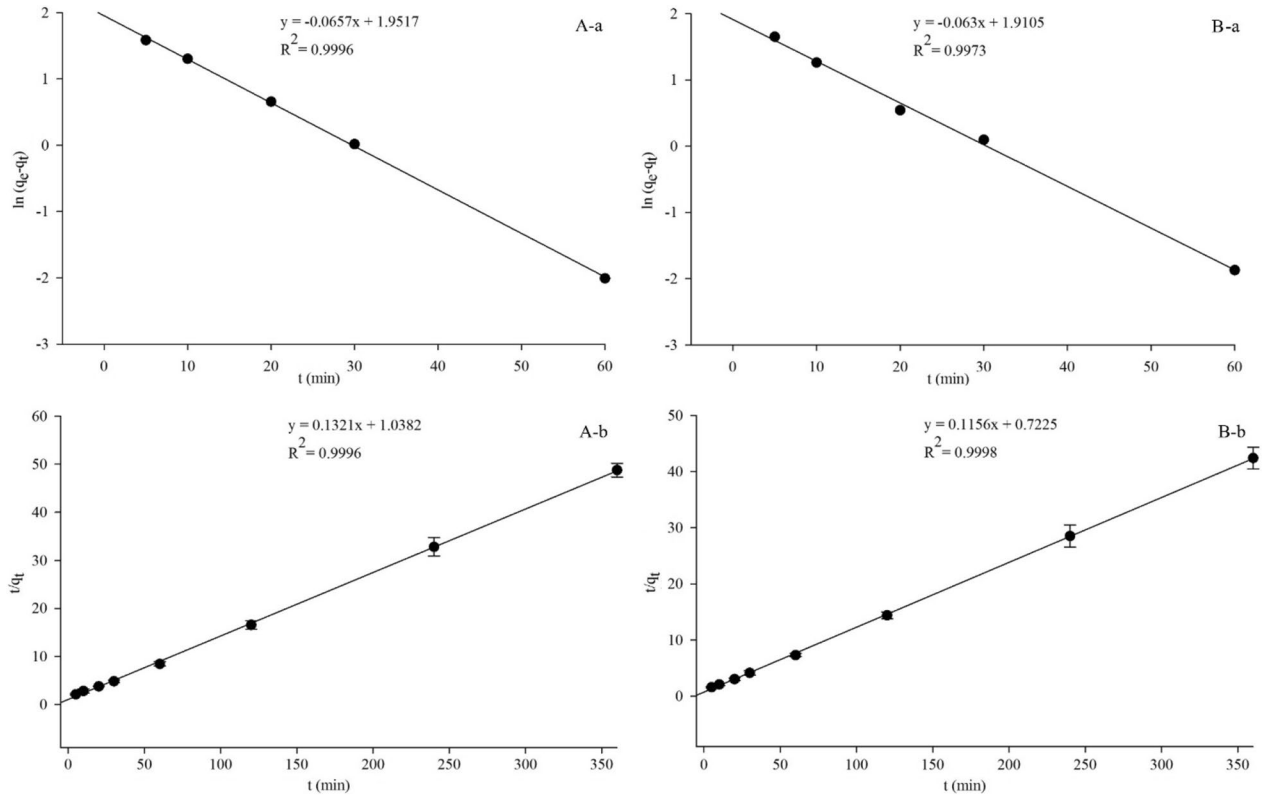

Fig. 5 Pseudo-first-order (**a**) and pseudo-second-order (**b**) kinetic plots of the living (**A**) and non-living (**B**) biomass of *Cupriavidus necator* GX_5

Table 3 Adsorption kinetic parameters of Cd (II) by live and dead biomass of *Cupriavidus necator* GX_5

Strain type	q_{max}(mg/g)	Pseudo-first-order			Pseudo-second-order		
		q_e(mg/g)	k_1	R^2	q(mg/g)	k_2	R^2
Live	7.27	7.04	0.0657	0.9967	7.57	0.0168	0.9996
Dead	8.36	6.76	0.0630	0.9973	8.65	0.0185	0.9998

both biosorbents. However, the predicted q_e was lower than the q_{max} of the experimental data in the pseudo-first-order model, especially for the non-living biomass, at 6.76 mg/g in comparison to 8.36 mg/g.

Febrianto et al. indicated that the adsorption process cannot fit the pseudo-first-order model if a large discrepancy occurs between the predicted q_e and the experimental q_{max} even if the plot had a high coefficient [60]. This result may be caused by the boundary layer or external resistance controlling at the beginning of the adsorption reaction, which was named as a time lag [61].

The predicted q_e (8.65 mg/g) in the pseudo-second order was close to q_{max} (6.76 mg/g) (Table 3.), which indicated that the pseudo-second-order kinetic model was a better fit in describing the adsorption process. This tendency suggests that the rate-limiting step may be chemisorption, complexation, coordination and/or chelation [62, 63].

Biosorption isotherm evaluation

Two widely used isotherm models, the Langmuir and Freundlich isotherm models, were applied for the analysis of the fit of data, which can determine the adsorption affinity and capacity of the biosorbents [64]. The Langmuir model is usually used for monolayer adsorption of specific homogenous sites, whereas the Freudlich model is highly suitable for heterogeneous adsorption types of different active sites [65].

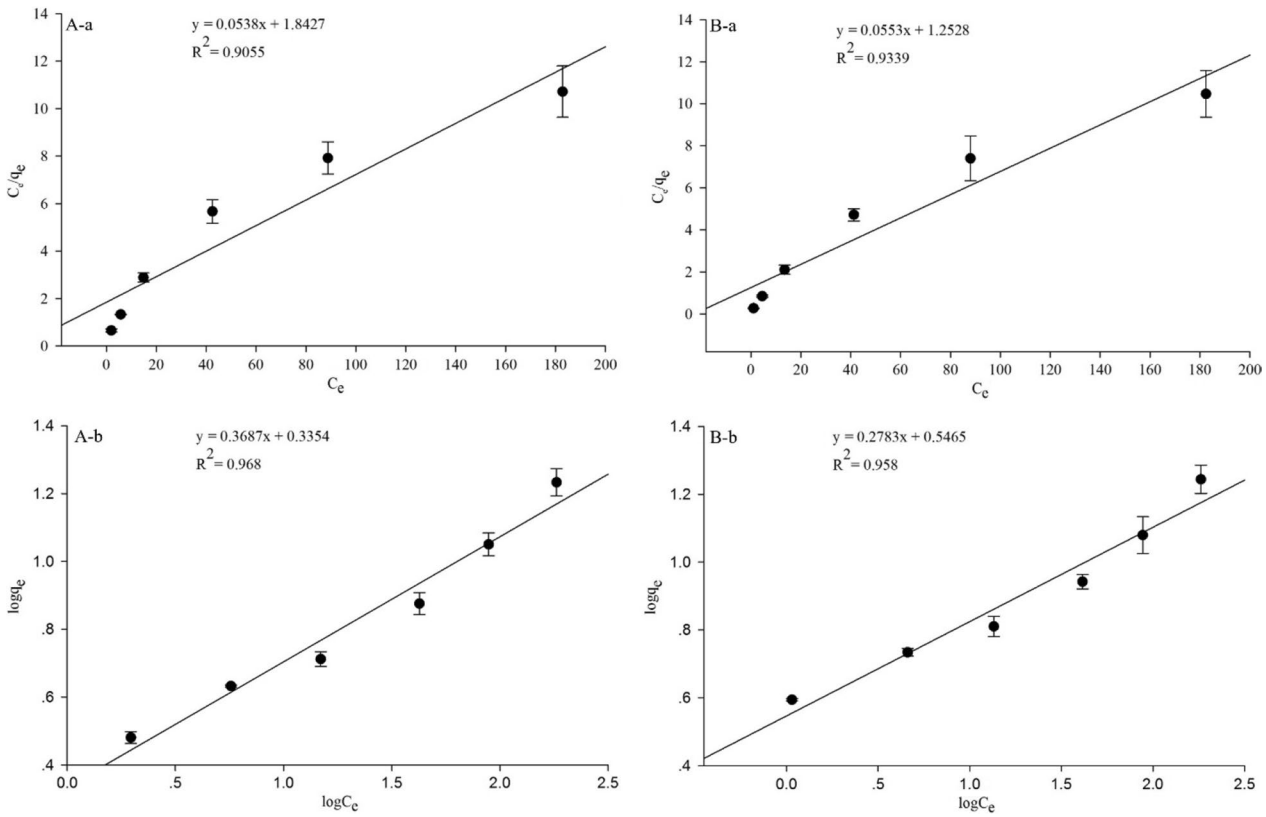

Fig. 6 Langmuir (**a**) and Freundlich (**b**) isotherm plots of the living (**A**) and non-living (**B**) biomass of *Cupriavidus necator* GX_5

Table 4 Langmuir and Freundlich biosorption constants of Cd (II) by live and dead biomass of *Cupriavidus necator* GX_5

Strain type	Langmuir isotherm				Freundlich isotherm		
	K_L	q_{max}(mg/g)	R_L	R^2	n	K_F	R^2
Live	0.0292	18.59	0.1462	0.9055	2.7122	2.1647	0.9680
Dead	0.0441	18.08	0.1017	0.9339	3.5932	3.5197	0.9580

The linear plots and model parameters are shown in Fig. 6; Table 4. We determined that the R^2 values in the Freundlich isotherm equation for Cd (II) adsorption by both living and non-living biosorbents were higher than those in the Langmuir model, indicating that the Freundlich isotherm model provided a better fit than the Langmuir isotherm model. This implied that the adsorption process of both biosorbents was heterogeneous and had multilayer adsorption.

The characteristics of the Freundlich equation are determined by the constants K_F and n. K_F is usually used to indicate the adsorption capacity of biosorbent to adsorbate; n means the adsorption strength, and the larger the n is, the stronger the reaction between the biosorbent and the adsorbate [66]. We discovered that the K_F value (3.5197) of non-living cells was larger than that (2.1647) of living cells in the Freundlich model (Table 4), indicating that the dead biomass had a higher Cd (II) adsorption capacity than the living biomass, which is also shown in Figs. 1 and 4; Table 3. This phenomenon agrees with experiments conducted by other investigators [67]. Meanwhile, the adsorption strength of the non-living biosorbent was stronger than that of the living biosorbent by comparing the n values of 3.5932 against 2.7122 from Table 4.

SEM and FT-IR analysis

In our previous investigation, the minimal inhibitory concentration of *C. necator* GX_5 for Cd (II) was 6 mM [21]. Furthermore, the higher the metal concentration, the more evident the results would be to some extent; thus, 100 mg/L of Cd (II) was used in the SEM and FT-IR characterisation of the adsorption process.

The surface morphology characterisation of the living and non-living biosorbents of *C. necator* GX_5 before and after the adsorption of Cd (II) was studied using

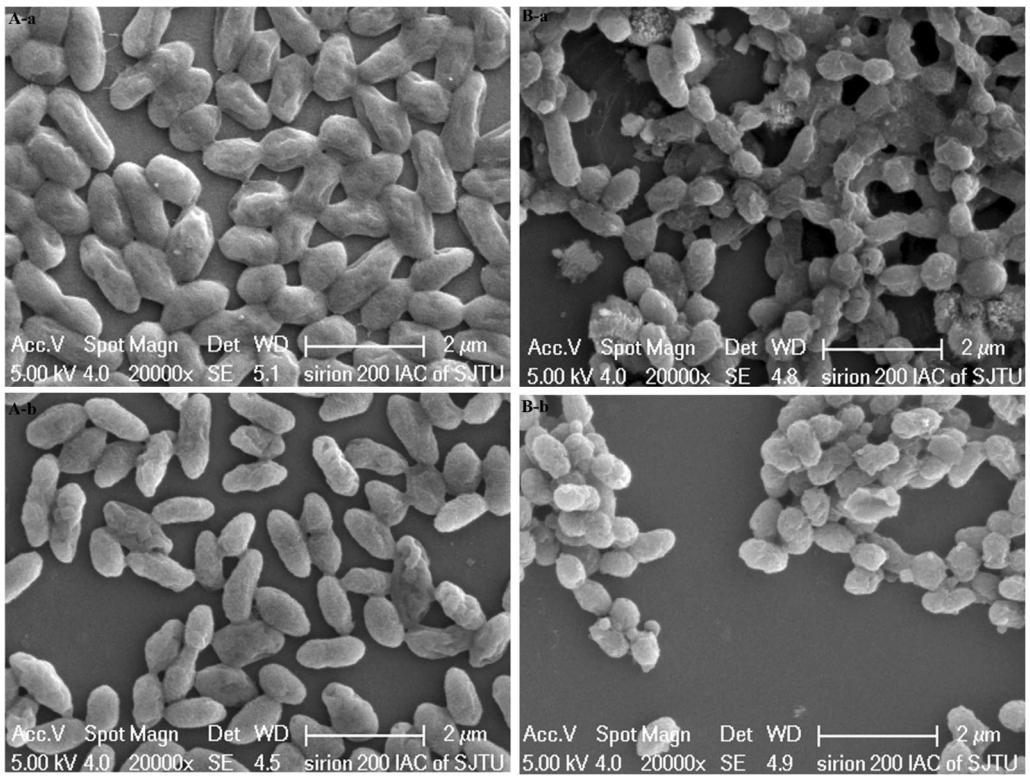

Fig. 7 SEM images of the living (**A**) and non-living (**B**) biomass of *Cupriavidus necator* GX_5 before (**a**) and after (**b**) adsorption

SEM, and the results are shown in Fig. 7. The surfaces of the living and non-living cells were smooth and invaginated before adsorption. In addition, the dead biomass seemed to clump. After loading with Cd (II), the invaginated parts were filled with particles and plumped, and the surface was coated with sediments. This phenomenon may be caused by the interaction of Cd (II) with microbial extracellular polymeric substances [68].

The functional groups on the cell surface were an important factor for absorbing metal ions. Changes in adsorption peaks indicate that the functional groups on the cell surface may have participated in the metal combination [69]. Therefore, the changes in the functional groups before and after adsorption with Cd (II) by the two types of biosorbents were surveyed using an FT-IR instrument. The infrared spectrum showed several different adsorption peaks, as displayed in Fig. 8. Before

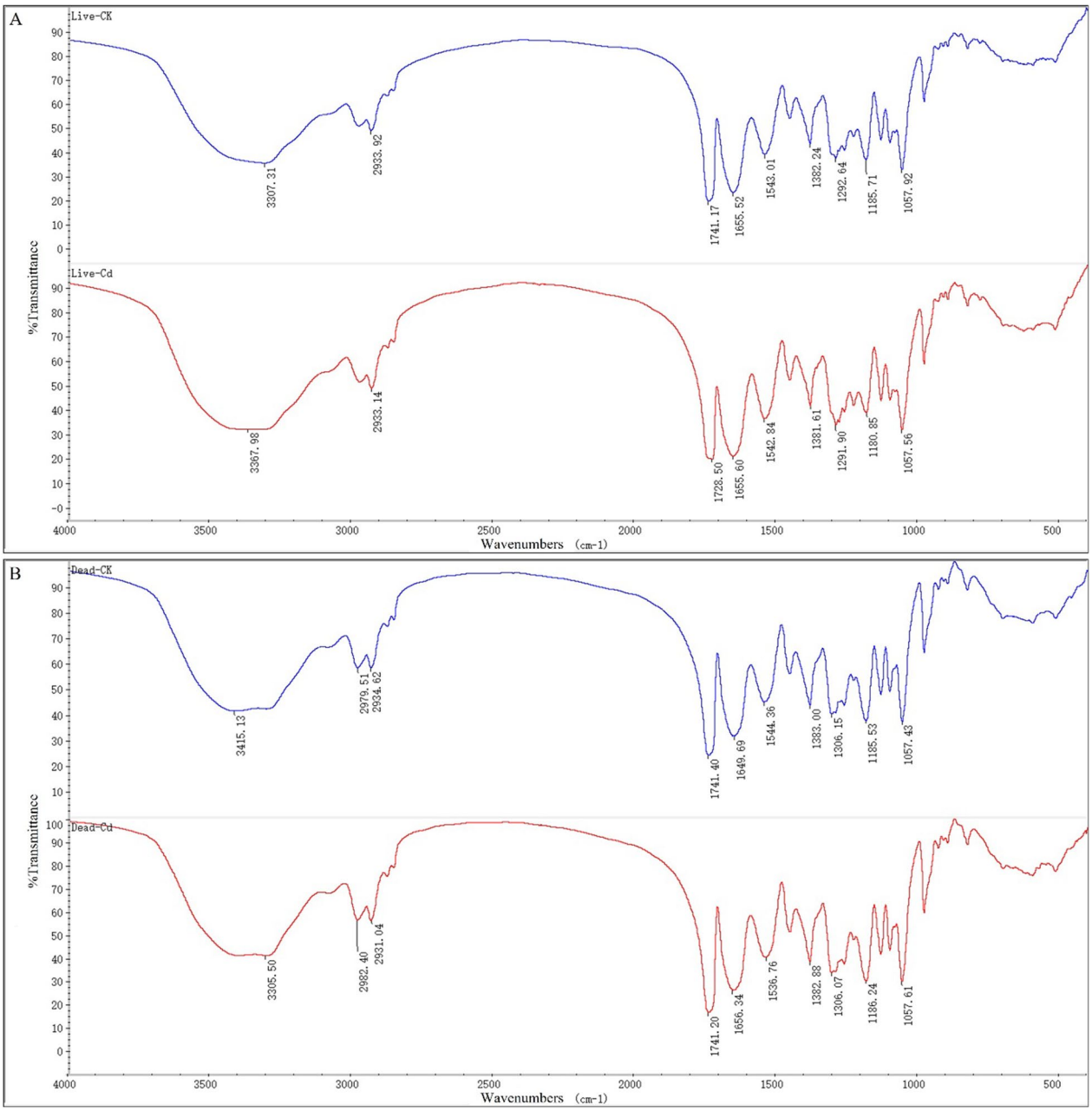

Fig. 8 FT-IR spectra of living (**A**) and non-living (**B**) biomass of *Cupriavidus necator* GX_5 before and after adsorption

Table 5 Main functional groups of Fourier Transform Infrared (FTIR) spectra before and after adsorption

Strain type	Before adsorption (cm^{-1})	After adsorption (cm^{-1})	Differences in shifts (cm^{-1})	Assignment
Living	3307.31	3367.98	60.67	stretching vibration of O–H and N–H of saccharide
	1741.17	1728.50	− 12.67	C=O stretching vibrations from lipids
	1185.71	1180.85	− 4.86	C–O and C–C stretching vibrations
Non-living	3415.13	3305.50	− 109.63	stretching vibration of O–H and N–H of saccharide
	2979.51	2982.40	2.89	C–H stretching vibrations
	2934.62	2931.04	− 3.58	asymmetric C–H stretching vibration
	1649.69	1656.34	6.65	stretching vibration of C=O(amide I)
	1544.36	1536.76	− 7.6	stretching vibration of C–N and deformation vibration of N–H (amide II)

adsorption, the characteristic peaks of the living and non-living biomass were similar, except that a new peak at 2979.51 cm^{-1} appeared for the non-living biosorbent, which was obviously very acute. Although the peaks were similar between the living and non-living biosorbents, the action mode performed differently after Cd (II) adsorption, as demonstrated in Table 5. Xu et al. [11] studied the characterisation of Cd (II) biosorption of the living and non-living biomass of *Pseudomonas* sp. 375, and their results are consistent with ours.

For the living biosorbent, the major spectrum bands shifted from 3307.31, 1741.17 and 1185.71 cm^{-1} before adsorption to 3367.98, 1728.50 and 1180.85 cm^{-1} after adsorption, representing the stretching vibrations of O–H and N–H of saccharides [70], stretching vibrations of C=O of lipids, and stretching vibrations of C–O and C–C, respectively [71] (Fig. 8A; Table 5). Regarding the non-living biomass loaded with and without Cd(II), the main offsets were from 3415.13, 2979.51, 2934.62, 1649.69 and 1544.36 cm^{-1} to 3305.50, 2982.40, 2931.04, 1656.34 and 1536.76 cm^{-1}, corresponding to the stretching vibrations of O–H and N–H [70], stretching vibrations of C–H [72], stretching vibrations of asymmetric C–H [73], stretching vibrations of C=O (amide I) [74], and stretching vibrations of C–N and deformation vibrations of N–H (amide II) [75], respectively (Fig. 8B; Table 5). All the above indicated that –OH, –NH, C=O, C–O and C–C groups might be involved in Cd (II) adsorption for living biosorbents, and –OH, –NH, C–H, C=O, C–N and N–H groups were associated with non-living biosorbents. Meanwhile, we determined that more functional groups participated in Cd (II) adsorption, which might partly explain why the adsorption capacity of non-living cells was higher than that of living cells.

Conclusions

In this study, the living and non-living biomass of *C. necator* GX_5, which is a previously isolated Cd-resistant strain, were evaluated for their adsorption capacity and/or removal efficiency of Cd (II). The pH, initial metal concentration, dosage and contact time significantly affected the reaction process. The maximum removal efficiency rates for the living and non-living biomass were 60.51% and 78.53%, respectively, at an optimum pH of 6, a dosage of 1 g/L and an initial Cd (II) concentration of 5 mg/L. The pseudo-second-order kinetic model was a better fit in describing the adsorption process. The Freundlich isotherm model provided a better fit than the Langmuir model for both the living and non-living biosorbents. SEM analysis verified the Cd (II) absorption on the cell surface. FT-IR observation suggested that the functional groups of –OH, –NH, C=O, C–O and C–C of the living biomass and the –OH, –NH, C–H, C=O, C–N and N–H groups of the non-living biomass might be responsible for Cd (II) adsorption. This work implied that non-living biosorbents were superior to living biosorbents in Cd (II)-adsorbing capacity and strength, which is a promising adsorbent in Cd (II)-contaminated environments.

Supplementary Information

The online version contains supplementary material available at https://doi.org/10.1186/s13065-023-00977-4.

Additional file 1: Figure S1. *Cupriavidus necator* GX_5 colonies grown on LB agar. **Table S1.** The effect of initial Cd concentration on adsorption capacity of *Cupriavidus necator* GX_5. **Table S2.** The effect of initial Cd concentration on removal efficiency of *Cupriavidus necator* GX_5. **Table S3.** The effect of biosorbent dosage on adsorption capacity of *Cupriavidus necator* GX_5. **Table S4.** The effect of biosorbent dosage on removal efficiency of *Cupriavidus necator* GX_5.

Acknowledgements

Authors are thankful to YH for SEM analysis and BSZ for FTIR spectra analysis (Instrumental Analysis Center of Shanghai Jiao Tong University, Shanghai, China). The authors are thankful to the anonymous reviewers for their comments.

Author contributions
XJL designed the experiments. QSX and QS performed the experiment and wrote the manuscript. XPL analyzed the data. JJK and LYL helped in experimental work and writing the manuscript. XJL, ZGZ and RGL helped in supervision, validation, manuscript editing and correction. All authors reviewed the manuscript.

Funding
This work was supported by National Natural Science Foundation of China (32260033), Science and Technology Research Project of Jiangxi Education Department (GJJ201619, GJJ201618) and Innovation and Entrepreneurship Training Program for College Students in Jiangxi Province (S202110417021). The funding body played no role in the design of the study and collection, analysis, interpretation of data, and in writing the manuscript.

Availability of data and materials
All data generated or analysed during this study are included in this published article [and its supplementary information files]. Raw data can be shared via correspondence upon reasonable request.

Declarations

Ethics approval and consent to participate
Not applicable.

Consent for publication
Not applicable.

Competing interests
The authors declare no competing interests.

Received: 29 December 2022 Accepted: 30 May 2023
Published online: 14 June 2023

References

1. Ali H, Khan E. What are heavy metals? Long-standing controversy over the scientific use of the term 'heavy metals'–proposal of a comprehensive definition. Toxicol Environ Chem. 2018;100:6–19. https://doi.org/10.1080/02772248.2017.1413652.
2. Cui L, Li J, Gao X, Tian B, Zhang J, Wang X, Liu Z. Human health ambient water quality criteria for 13 heavy metals and health risk assessment in Taihu Lake. Front Environ Sci Eng. 2022;16(4):41. https://doi.org/10.1007/s11783-021-1475-6.
3. Zhou W, Liu D, Kong W, Zhang Y. Bioremoval and recovery of cd (II) by *Pseudoalteromonas* sp. SCSE709-6: comparative study on growing and grown cells. Bioresource Technol. 2014;165:145–51. https://doi.org/10.1016/j.biortech.2014.01.119.
4. Plöhn M, Escudero-Oñate C, Funk C. Biosorption of Cd (II) by nordic microalgae: tolerance, kinetics and equilibrium studies. Algal Res. 2021;59:102471. https://doi.org/10.1016/j.algal.2021.102471.
5. Mathialagan T, Viraraghavan T. Adsorption of cadmium from aqueous solutions by perlite. J Hazard Mater. 2002;94:291–303. https://doi.org/10.1016/S0304-3894(02)00084-5.
6. Vilela PB, Matias CA, Dalalibera A, Becegato VA, Paulino AT. Polyacrylic acid-based and chitosan-based hydrogels for adsorption of cadmium: equilibrium isotherm, kinetic and thermodynamic studies. J Environ Chem Eng. 2019;7:103327. https://doi.org/10.1016/j.jece.2019.103327.
7. Bimonte VM, Besharat ZM, Antonioni A, Cella V, Lenzi A, Ferretti E, Migliaccio S. The endocrine disruptor cadmium: a new player in the pathophysiology of metabolic diseases. J Endocrinol Invest. 2021;44:1363–77. https://doi.org/10.1007/s40618-021-01502-x.
8. Hadiani MR, Khosravi-Darani K, Rahimifard N, Younesi H. Assessment of mercury biosorption by *Saccharomyces cerevisiae*: response surface methodology for optimization of low hg (II) concentrations. J Environ Chem Eng. 2018;6:4980–7. https://doi.org/10.1016/j.jece.2018.07.034.
9. Acién FG, Gómez-Serrano C, Morales-Amaral MdM, Fernández-Sevilla JM, Molina-Grima E. Wastewater treatment using microalgae: how realistic a contribution might it be to significant urban wastewater treatment? Appl Microbiol Biot. 2016;100:9013–22. https://doi.org/10.1007/s00253-016-7835-7.
10. Yin K, Wang Q, Lv M, Chen L. Microorganism remediation strategies towards heavy metals. Chem Eng J. 2019;360:1553–63. https://doi.org/10.1016/j.cej.2018.10.226.
11. Xu S, Xing Y, Liu S, Hao X, Chen W, Huang Q. Characterization of Cd^{2+} biosorption by *Pseudomonas* sp. strain 375, a novel biosorbent isolated from soil polluted with heavy metals in Southern China. Chemosphere. 2020;240:124893. https://doi.org/10.1016/j.chemosphere.2019.124893.
12. Yu R, Chai H, Yu Z, Wu X, Liu Y, Shen L, Li J, Ye J, Liu D, Ma T. Behavior and mechanism of cesium biosorption from aqueous solution by living *Synechococcus* PCC7002. Microorganisms. 2020;8:491. https://doi.org/10.3390/microorganisms8040491.
13. Khan I, Ali M, Aftab M, Shakir S, Qayyum S, Haleem KS, Tauseef I. Mycoremediation: a treatment for heavy metal-polluted soil using indigenous metallotolerant fungi. Environ Monit Assess. 2019;191:1–15. https://doi.org/10.1007/s10661-019-7781-9.
14. Rangabhashiyam S, Balasubramanian P. Characteristics, performances, equilibrium and kinetic modeling aspects of heavy metal removal using algae. Bioresource Technol Rep. 2019;5:261–79. https://doi.org/10.1016/j.biteb.2018.07.009.
15. Priyadarshanee M, Das S. Biosorption and removal of toxic heavy metals by metal tolerating bacteria for bioremediation of metal contamination: a comprehensive review. J Environ Chem Eng. 2021;9:104686. https://doi.org/10.1016/j.jece.2020.104686.
16. Priya A, Gnanasekaran L, Dutta K, Rajendran S, Balakrishnan D, Soto-Moscoso M. Biosorption of heavy metals by microorganisms: evaluation of different underlying mechanisms. Chemosphere. 2022;307:135957. https://doi.org/10.1016/j.chemosphere.2022.135957.
17. Zhu W, Xu X, Xia L, Huang Q, Chen W. Comparative analysis of mechanisms of Cd^{2+} and Ni^{2+} biosorption by living and nonliving *Mucoromycote* sp. XLC Geomicrobiol J. 2016;33:274–82. https://doi.org/10.1080/01490451.2015.1052114.
18. Lin Y, Wang X, Wang B, Mohamad O, Wei G. Bioaccumulation characterization of zinc and cadmium by *Streptomyces zinciresistens*, a novel actinomycete. Ecotox Environ Safe. 2012;77:7–17. https://doi.org/10.1016/j.ecoenv.2011.09.016.
19. Huang F, Dang Z, Guo C-L, Lu G-N, Gu RR, Liu H-J, Zhang H. Biosorption of Cd (II) by live and dead cells of *Bacillus cereus* RC-1 isolated from cadmium-contaminated soil. Colloid Surf B. 2013;107:11–8. https://doi.org/10.1016/j.colsurfb.2013.01.062.
20. Gadd GM. Biosorption: critical review of scientific rationale, environmental importance and significance for pollution treatment. J Chem Technol Biotechnol. 2009;84:13–28. https://doi.org/10.1002/jctb.1999.
21. Li X, Yan Z, Gu D, Li D, Tao Y, Zhang D, Su L, Ao Y. Characterization of cadmium-resistant rhizobacteria and their promotion effects on *Brassica napus* growth and cadmium uptake. J Basic Microb. 2019;59:579–90. https://doi.org/10.1002/jobm.201800656.
22. Li X, Li D, Yan Z, Ao Y. Adsorption of cadmium by live and dead biomass of plant growth-promoting rhizobacteria. RSC Adv. 2018;8:33523–33. https://doi.org/10.1039/c8ra06758a.
23. Li X, Li D, Yan Z, Ao Y. Biosorption and bioaccumulation characteristics of cadmium by plant growth-promoting rhizobacteria. RSC Adv. 2018;8:30902–11. https://doi.org/10.1039/C8RA06270F.
24. Navarta L, Calvo J, Calvente V, Benuzzi D, Sanz M. Freezing and freeze-drying of the bacterium *Rahnella aquatilis* BNM 0523: study of protecting agents, rehydration media and freezing temperatures. Lett Appl Microbiol. 2011;53:565–71. https://doi.org/10.1111/j.1472-765X.2011.03150.x.
25. He T, Hua J-q, Chen R-p, Yu L. Adsorption characteristics of methylene blue by a dye-degrading and extracellular polymeric substance-producing strain. J Environ Manage. 2021;288:112446. https://doi.org/10.1016/j.jenvman.2021.112446.
26. Demirbas A, Pehlivan E, Gode F, Altun T, Arslan G. Adsorption of Cu (II), zn (II), ni (II), pb (II), and cd (II) from aqueous solution on amberlite IR-120 synthetic resin. J Colloid Interf Sci. 2005;282:20–5. https://doi.org/10.1016/j.jcis.2004.08.147.
27. Akl MA, Hashem MA, Ismail MA, Abdelgalil DA. Novel diaminoguanidine functionalized cellulose: synthesis, characterization, adsorption characteristics and application for ICP-AES determination of copper (II), mercury

(II), lead (II) and cadmium (II) from aqueous solutions. BMC Chem. 2022;16(1):65. https://doi.org/10.1186/s13065-022-00857-3.
28. Ezeonuegbu BA, Machido DA, Whong CM, Japhet WS, Alexiou A, Elazab ST, Qusty N, Yaro CA, Batiha GE-S. Agricultural waste of sugarcane bagasse as efficient adsorbent for lead and nickel removal from untreated wastewater: Biosorption, equilibrium isotherms, kinetics and desorption studies. Biotechnol Rep. 2021;30:e00614. https://doi.org/10.1016/j.btre.2021.e00614.
29. Lim J-H, Kang H-M, Kim L-H, Ko S-O. Removal of heavy metals by sawdust adsorption: equilibrium and kinetic studies. Environ Eng Res. 2008;13:79–84. https://doi.org/10.4491/eer.2008.13.2.079.
30. Kanamarlapudi SLRK, Muddada S. Biosorption of iron (II) by *Lactobacillus fermentum* from aqueous solutions. P J Environ Stud. 2020;29:1659–70. https://doi.org/10.15244/pjoes/103443.
31. Tomczyk A, Sokołowska Z, Boguta P. Biomass type effect on biochar surface characteristic and adsorption capacity relative to silver and copper. Fuel. 2020;278:118168. https://doi.org/10.1016/j.fuel.2020.118168.
32. Xiao Y, Luo R, Ji Y, Li S, Hu H, Zhang X. Removal of copper (II) from Aqueous Environment using Silk Sericin-Derived Carbon. Int J Mol Sci. 2022;23:11202. https://doi.org/10.3390/ijms231911202.
33. Jonas B. Decontamination of cadmium (II) from synthetic wastewater onto shea fruit shell biomass. Appl Water Sci. 2021;11:84. https://doi.org/10.1007/s13201-021-01416-2.
34. Oves M, Khan M, Qari H. Ensifer adhaerens for heavy metal bioaccumulation, biosorption, and phosphate solubilization under metal stress condition. J Taiwan Inst Chem E. 2017;80:540–52. https://doi.org/10.1016/j.jtice.2017.08.026.
35. Xu X, Xia L, Huang Q, Gu J-D, Chen W. Biosorption of cadmium by a metal-resistant filamentous fungus isolated from chicken manure compost. Environ Technol. 2012;33:1661–70. https://doi.org/10.1080/09593330.2011.641591.
36. Bharti SK, Kumar N. Kinetic study of lead (Pb^{2+}) removal from battery manufacturing wastewater using bagasse biochar as biosorbent. Appl Water Sci. 2018;8:1–13. https://doi.org/10.1007/s13201-018-0765-z.
37. Huang W, Liu Z. Biosorption of Cd (II)/Pb (II) from aqueous solution by biosurfactant-producing bacteria: isotherm kinetic characteristic and mechanism studies. Colloid Surf B. 2013;105:113–9. https://doi.org/10.1016/j.colsurfb.2012.12.040.
38. Limcharoensuk T, Sooksawat N, Sumarnrote A, Awutpet T, Kruatrachue M, Pokethitiyook P, Auesukaree C. Bioaccumulation and biosorption of Cd^{2+} and Zn^{2+} by bacteria isolated from a zinc mine in Thailand. Ecotox Environ Safe. 2015;122:322–30. https://doi.org/10.1016/j.ecoenv.2015.08.013.
39. Li D, Zhou L. Adsorption of heavy metal tolerance strains to Pb^{2+} and Cd^{2+} in wastewater. Environ Sci Pollut R. 2018;25:32156–62. https://doi.org/10.1007/s11356-018-2988-9.
40. Yuan W, Cheng J, Huang H, Xiong S, Gao J, Zhang J, Feng S. Optimization of cadmium biosorption by *Shewanella putrefaciens* using a Box-Behnken design. Ecotox Environ Safe. 2019;175:138–47. https://doi.org/10.1016/j.ecoenv.2019.03.057.
41. Vijayaraghavan K, Yun Y-S. Bacterial biosorbents and biosorption. Biotechnol Adv. 2008;26:266–91. https://doi.org/10.1016/j.biotechadv.2008.02.002.
42. Hassan M, Naidu R, Du J, Liu Y, Qi F. Critical review of magnetic biosorbents: their preparation, application, and regeneration for wastewater treatment. Sci Total Environ. 2020;702:134893. https://doi.org/10.1016/j.scitotenv.2019.134893.
43. Sheikh Z, Amin M, Khan N, Khan MN, Sami SK, Khan SB, Hafeez I, Khan SA, Bakhsh EM, Cheng CK. Potential application of *Allium Cepa* seeds as a novel biosorbent for efficient biosorption of heavy metals ions from aqueous solution. Chemosphere. 2021;279:130545. https://doi.org/10.1016/j.chemosphere.2021.130545.
44. Lu N, Hu T, Zhai Y, Qin H, Aliyeva J, Zhang H. Fungal cell with artificial metal container for heavy metals biosorption: equilibrium, kinetics study and mechanisms analysis. Environ Res. 2020;182:109061. https://doi.org/10.1016/j.envres.2019.109061.
45. Kanamarlapudi SLRK, Muddada S. Structural changes of Biomass on Biosorption of Iron (II) from Aqueous Solutions: Isotherm and Kinetic Studies. Pol J Microbiol. 2019;68:549–58. https://doi.org/10.33073/pjm-2019-057.
46. Nithya K, Sathish A, Kumar PS, Ramachandran T. Fast kinetics and high adsorption capacity of green extract capped superparamagnetic iron oxide nanoparticles for the adsorption of Ni (II) ions. J Ind Eng Chem. 2018;365:230–41. https://doi.org/10.1016/j.jiec.2017.10.028.
47. Lo S-F, Wang S-Y, Tsai M-J, Lin L-D. Adsorption capacity and removal efficiency of heavy metal ions by Moso and Ma bamboo activated carbons. Chem Eng Res Des. 2012;90:1397–406. https://doi.org/10.1016/j.cherd.2011.11.020.
48. Tran TH, Okabe H, Hidaka Y, Hara K. Equilibrium and kinetic studies for silver removal from aqueous solution by hybrid hydrogels. J Hazard Mater. 2019;365:237–44. https://doi.org/j.jhazmat.2018.11.008.
49. Vishan I, Saha B, Sivaprakasam S, Kalamdhad A. Evaluation of cd (II) biosorption in aqueous solution by using lyophilized biomass of novel bacterial strain *Bacillus badius* AK: Biosorption kinetics, thermodynamics and mechanism. Environ Technol Inno. 2019;14:100323. https://doi.org/10.1016/j.eti.2019.100323.
50. Shrestha R, Ban S, Devkota S, Sharma S, Joshi R, Tiwari AP, Kim HY, Joshi MK. Technological trends in heavy metals removal from industrial wastewater: a review. J Environ Chem Eng. 2021;9:105688. https://doi.org/10.1016/j.jece.2021.105688.
51. Tahoon MA, Siddeeg SM, Salem Alsaiari N, Mnif W, Ben Rebah F. Effective heavy metals removal from water using nanomaterials: a review. Processes. 2020;8:645. https://doi.org/10.3390/pr8060645.
52. Pang C, Liu Y-H, Cao X-H, Li M, Huang G-L, Hua R, Wang C-X, Liu Y-T, An X-F. Biosorption of uranium (VI) from aqueous solution by dead fungal biomass of *Penicillium citrinum*. Chem Eng J. 2011;170:1–6. https://doi.org/10.1016/j.cej.2010.10.068.
53. Li H, Lin Y, Guan W, Chang J, Xu L, Guo J, Wei G. Biosorption of Zn (II) by live and dead cells of *Streptomyces ciscaucasicus* strain CCNWHX 72 – 14. J Hazard Mater. 2010;179:151–9. https://doi.org/10.1016/j.jhazmat.2010.02.072.
54. Singh S, Kumar V, Gupta P, Ray M, Kumar A. The synergy of mercury biosorption through *Brevundimonas* sp. IITISM22: kinetics, isotherm, and thermodynamic modeling. J Hazard Mater. 2021;415:125653. https://doi.org/10.1016/j.jhazmat.2021.125653.
55. Bulgariu D, Bulgariu L. Equilibrium and kinetics studies of heavy metal ions biosorption on green algae waste biomass. Bioresource Technol. 2012;103:489–93. https://doi.org/10.1016/j.biortech.2011.10.016.
56. Simonin J-P. On the comparison of pseudo-first order and pseudo-second order rate laws in the modeling of adsorption kinetics. Chem Eng J. 2016;300:254–63. https://doi.org/10.1016/j.cej.2016.04.079.
57. Ezzati R. Derivation of pseudo-first-order, pseudo-second-order and modified pseudo-first-order rate equations from Langmuir and Freundlich isotherms for adsorption. Chem Eng J. 2020;392:123705. https://doi.org/10.1016/j.cej.2019.123705.
58. Mahmoud ME, Saleh MM, Zaki MM, Nabil GM. A sustainable nanocomposite for removal of heavy metals from water based on crosslinked sodium alginate with iron oxide waste material from steel industry. J Environ Chem Eng. 2020;8(4):104015. https://doi.org/10.1016/j.jece.2020.104015.
59. Greluk M, Hubicki Z. Kinetics, isotherm and thermodynamic studies of Reactive Black 5 removal by acid acrylic resins. Chem Eng J. 2010;162:919–26. https://doi.org/10.1016/j.cej.2010.06.043.
60. Febrianto J, Kosasih AN, Sunarso J, Ju Y-H, Indraswati N, Ismadji S. Equilibrium and kinetic studies in adsorption of heavy metals using biosorbent: a summary of recent studies. J Hazard Mater. 2009;162:616–45. https://doi.org/10.1016/j.jhazmat.2008.06.042.
61. Vijayaraghavan K, Palanivelu K, Velan M. Biosorption of copper (II) and cobalt (II) from aqueous solutions by crab shell particles. Bioresource Technol. 2006;97:1411–9. https://doi.org/10.1016/j.biortech.2005.07.001.
62. Wang Z, Lu N, Cao X, Li Q, Gong S, Lu P, Feike T. Interactions between cr (VI) and the hydrochar: the electron transfer routes, adsorption mechanisms, and the accelerating effects of wood vinegar. Sci Total Environ. 2023;863:160957. https://doi.org/10.1016/j.scitotenv.2022.160957.
63. Majumder R, Sheikh L, Naskar A, Mukherjee M, Tripathy S. Depletion of cr (VI) from aqueous solution by heat dried biomass of a newly isolated fungus *arthrinium malaysianum*: a mechanistic approach. Sci Rep-UK. 2017;7:1–15. https://doi.org/10.1038/s41598-017-10160-0.
64. Liu J, Zhou R, Yu J, Guo L, Li X, Xiao C, Hou H, Chi R, Feng G. Simultaneous removal of lead, manganese, and copper released from the copper

tailings by a novel magnetic modified biosorbent. J Environ Manage. 2022;322:116157. https://doi.org/10.1016/j.jenvman.2022.116157.
65. Kalam S, Abu-Khamsin SA, Kamal MS, Patil S. Surfactant adsorption isotherms: a review. ACS Omega. 2021;6:32342–8. https://doi.org/10.1021/acsomega.1c04661.
66. Sahu S, Pahi S, Tripathy S, Singh SK, Behera A, Sahu UK, Patel RK. Adsorption of methylene blue on chemically modified lychee seed biochar: dynamic, equilibrium, and thermodynamic study. J Mol Liq. 2020;315:113743. https://doi.org/10.1016/j.molliq.2020.113743.
67. Hu X, Cao J, Yang H, Li D, Qiao Y, Zhao J, Zhang Z, Huang L. Pb^{2+} biosorption from aqueous solutions by live and dead biosorbents of the hydrocarbon-degrading strain *Rhodococcus* sp. HX-2. PLoS ONE. 2020;15:e0226557. https://doi.org/10.1371/journal.pone.0226557.
68. Zhang P, Chen Y-P, Peng M-W, Guo J-S, Shen Y, Yan P, Zhou Q-H, Jiang J, Fang F. Extracellular polymeric substances dependence of surface interactions of *Bacillus subtilis* with Cd^{2+} and Pb^{2+}: an investigation combined with surface plasmon resonance and infrared spectra. Colloid Surf B. 2017;154:357–64. https://doi.org/10.1016/j.colsurfb.2017.03.046.
69. Pabst MW, Miller CD, Dimkpa CO, Anderson AJ, McLean JE. Defining the surface adsorption and internalization of copper and cadmium in a soil bacterium, *Pseudomonas putida*. Chemosphere. 2010;81:904–10. https://doi.org/10.1016/j.chemosphere.2010.07.069.
70. Li J, Liu Y-R, Zhang L-M, He J-Z. Sorption mechanism and distribution of cadmium by different microbial species. J Environ Manage. 2019;237:552–9. https://doi.org/10.1016/j.jenvman.2019.02.057.
71. Kasprzyk I, Depciuch J, Grabek-Lejko D, Parlinska-Wojtan M. FTIR-ATR spectroscopy of pollen and honey as a tool for unifloral honey authentication. The case study of rape honey. Food Control. 2018;84:33–40. https://doi.org/10.1016/j.foodcont.2017.07.015.
72. Hasan A, Pandey LM. Kinetic studies of attachment and re-orientation of octyltriethoxysilane for formation of self-assembled monolayer on a silica substrate. Mat Sci Eng. 2016;68:423–9. https://doi.org/10.1016/j.msec.2016.06.003.
73. El-Bahy G. FTIR and Raman spectroscopic study of Fenugreek (*Trigonella foenum graecum* L.) seeds. J Appl Spectrosc. 2005;72:111–6. https://doi.org/10.1007/s10812-005-0040-6.
74. Masoumi F, Khadivinia E, Alidoust L, Mansourinejad Z, Shahryari S, Safaei M, Mousavi A, Salmanian A-H, Zahiri HS, Vali H. Nickel and lead biosorption by *Curtobacterium* sp. FM01, an indigenous bacterium isolated from farmland soils of northeast Iran. J Environ Chem Eng. 2016;4:950–7. https://doi.org/10.1016/j.jece.2015.12.025.
75. Huang H, Jia Q, Jing W, Dahms H-U, Wang L. Screening strains for microbial biosorption technology of cadmium. Chemosphere. 2020;251:126428. https://doi.org/10.1016/j.chemosphere.2020.126428.

Publisher's Note